

Mass spectra and decay properties of the higher excited ρ mesons

Xue-Chao Feng,¹ Zheng-Ya Li,² De-Min Li,^{2,*} Qin-Tao Song,^{2,†} En Wang,^{2,‡} and Wen-Cheng Yan^{2,§}

¹College of Physics and Electronic Engineering, Zhengzhou University of Light Industry, Zhengzhou 450002, China

²School of Physics and Microelectronics, Zhengzhou University, Zhengzhou, Henan 450001, China

(Dated: June 22, 2022)

Although there are some experimental hints for the higher excited ρ mesons, our knowledge of their properties is much poor theoretically. Based on our recent work about excited ρ mesons [Phys.Rev.D104(2021)034013], we present the mass spectra and decay properties of the higher excited ρ mesons with the modified Godfrey-Isgur quark model and the 3P_0 strong decay model, and compare our predictions with the experimental hints, which should be helpful to search for these higher excited ρ mesons.

PACS numbers: 14.40.Be, 13.25.Jx

I. INTRODUCTION

In the last decades, a large number of light vector mesons with mass below 2.4 GeV have been reported experimentally [1–7], and a lot of research works have been conducted theoretically based on these experimental data [8–13]. These experimental and theoretical studies are crucial to deepen our understanding of the light vector mesons. In addition, the higher excited light vector mesons above 2.4 GeV play an important role in the processes involving the baryon anti-baryon interactions [14]. However, there are few theoretical and experimental studies on the higher excited light vector mesons, so it is necessary to study their properties, which should be helpful to search for them experimentally.

Recently, we have studied the mass spectra and strong decay properties of the excited ρ mesons $Y(2040)/\rho(2000)$, $\rho(1900)$, and $\rho(2150)$ with the modified Godfrey-Isgur quark model (MGI) including the screening effects and the 3P_0 strong decay model, and found that they can be assigned as $\rho(2^3D_1)$, $\rho(3^3S_1)$, and $\rho(4^3S_1)$, respectively [15]. We have also shown the screening effects are crucial to promote theoretical descriptions of the masses of the observed excited ρ mesons, as shown in Fig. 2 of Ref. [15]. We predict that the $Y(2040)$ mainly decays to $\pi\pi$ and $\pi\omega$, which is in good agreement with the measurements of the processes $p\bar{p} \rightarrow \pi\pi$ and $e^+e^- \rightarrow \omega\pi$ [5, 16]. For $\rho(1900)$, the predicted main decay modes are $\pi\omega$ and $a_2(1320)\pi$, which is also in consistent with the experimental measurements [3]. For $\rho(2150)$, its main decay modes are expected to be $\pi\pi$, $\pi\omega(1420)(\rightarrow 6\pi)$, and $\pi a_2(1320)(\rightarrow 6\pi)$, consistent with the experimental results [3]. Based on the successful description of the excited mesons $Y(2040)/\rho(2000)$, $\rho(1900)$, and $\rho(2150)$, we would like to extend our study to the higher excited ρ mesons with masses above 2.4 GeV in this work.

Although the higher excited ρ mesons above 2.4 GeV have not been reported experimentally, there exist some hints of them in the experimental measurements. For instance, in 2002, Anisovich *et al.* analyzed experimental data of the process $p\bar{p} \rightarrow \omega\eta\pi^0$ measured by the Crystal Barrel Collaboration, and showed that there exists a peak structure with $J^{PC} = 1^{--}$ around 2.4 GeV [17]. Later in 2006, the *BABAR* Collaboration reported the $\omega\pi^+\pi^-\pi^0$ energy-dependent reaction cross section, as shown in Fig. 18 of Ref. [18], where the blue data points correspond to the cross section data of the process $e^+e^- \rightarrow \omega\pi^+\pi^-\pi^0$. From Fig. 18 of Ref. [18], one can easily find a peak around 2.6 GeV, which may be the higher excited ρ meson according to the G parity conservation.

In 2007, the *BABAR* Collaboration presented the cross section of the process $e^+e^- \rightarrow K^+K^-\pi^+\pi^-\pi^0$, where there is a peak structure around 2.5 GeV [19]. The analysis of the *BABAR* measurements within the Vector Meson Dominance model shows the existences of the $\rho(1900)$ and another resonance with mass of $M = 2550 \pm 13$ MeV and width of $\Gamma = 209 \pm 26$ MeV [20], where the latter one is expected to have the same quantum numbers as $\rho(1900)$. In addition, the cross sections of $e^+e^- \rightarrow \eta'\pi^+\pi^-$ and $e^+e^- \rightarrow f_1(1285)\pi^+\pi^-$ processes reported by *BABAR* indicate that there exist some structures around 2.5 GeV, and it is difficult to claim the existences of new resonances due to the insufficient data statistics [19].

In a word, there exist some hints of the higher excited ρ mesons according to the above experimental measurements, as pointed out in Ref. [21], and the existences of the higher excited ρ mesons above 2.4 GeV need to be confirmed by more precise experimental measurements in future. The theoretical predictions for their mass spectra and decay properties are crucial to search for them experimentally. Thus, we will study the mass spectra and decay properties of the higher excited ρ mesons above 2.4 GeV with the MGI model and 3P_0 strong decay model, as used in our previous work [15].

The organization of this paper is as follows. First we introduce the MGI model and the 3P_0 model in Sec. II and Sec. III, respectively. Then we present the numeri-

* lidm@zzu.edu.cn

† songqintao@zzu.edu.cn

‡ wangen@zzu.edu.cn

§ yanwc@zzu.edu.cn

cal results of the mass spectra and strong decays for the higher excited ρ mesons in Sec. IV. Finally a short summary is given in Sec. V.

II. RELATIVISTIC QUARK MODEL

The Godfrey-Isgure relativistic quark model (GI model) was proposed in 1985 by Godfrey and Isgur [22], and is widely used in describing the mass spectra of mesons [23–25], especially for the lower excited mesons. However, the masses of the higher excited mesons measured by experiments are much lower than the predictions of the GI model. Many studies show that the screening effects play an important role in studying the higher radial and orbital excited mesons [26, 27]. First we present a brief introduction of the GI model, and the MGI model that includes the screening effects.

A. GI model

Within the GI model, the Hamiltonian of the meson's internal interaction can be written as [22],

$$\tilde{H} = \sqrt{m_1^2 + \mathbf{p}^2} + \sqrt{m_2^2 + \mathbf{p}^2} + \tilde{V}_{\text{eff}}(\mathbf{p}, \mathbf{r}), \quad (1)$$

where m_1 and m_2 denote the masses of quark and antiquark in the meson, respectively, $\mathbf{p} = \mathbf{p}_1 = -\mathbf{p}_2$ is the center-of-mass momentum, and \mathbf{r} corresponds to the spatial coordinate. The $\tilde{V}_{\text{eff}}(\mathbf{p}, \mathbf{r})$ is the effective potential between quark and antiquark, and can be expressed as follows in the non-relativistic limit,

$$V_{\text{eff}}(r) = H^{\text{conf}} + H^{\text{hyp}} + H^{\text{so}}, \quad (2)$$

where H^{conf} is spin-independent potential, includes the spin-independent linear confinement and Coulomb-type interaction,

$$\begin{aligned} H^{\text{conf}} &= \left[-\frac{3}{4}(c + br) + \frac{\alpha_s(r)}{r} \right] \mathbf{F}_1 \cdot \mathbf{F}_2 \\ &= S(r) + G(r), \end{aligned} \quad (3)$$

where $\langle \mathbf{F}_1 \cdot \mathbf{F}_2 \rangle = -4/3$ for a meson. $\alpha_s(Q^2)$ is the running coupling constant of QCD, which depends on the energy scale Q . $\alpha_s(Q^2)$ is divergent at low Q region. The authors of Ref. [22] assume that $\alpha_s(Q^2)$ saturates as $\alpha_s(Q^2 = 0) = \alpha_s^{\text{critical}}$, which is regarded as a parameter to be determined by fitting to experimental data. $\alpha_s(r)$ is obtained from $\alpha_s(Q^2)$ by using Fourier transform, where r is the relative distance between quark and antiquark. H^{hyp} denotes the color-hyperfine interaction,

$$\begin{aligned} H^{\text{hyp}} &= -\frac{\alpha_s(r)}{m_1 m_2} \left[\frac{1}{r^3} \left(\frac{3\mathbf{S}_1 \cdot \mathbf{r} \mathbf{S}_2 \cdot \mathbf{r}}{r^2} - \mathbf{S}_1 \cdot \mathbf{S}_2 \right) \right. \\ &\quad \left. + \frac{8\pi}{3} \mathbf{S}_1 \cdot \mathbf{S}_2 \delta^3(\mathbf{r}) \right] \mathbf{F}_1 \cdot \mathbf{F}_2. \end{aligned} \quad (4)$$

H^{so} is the spin-orbit interaction which contains the color-magnetic term $H^{\text{so(cm)}}$ and the Thomas-precession term $H^{\text{so(tp)}}$,

$$H^{\text{so}} = H^{\text{so(cm)}} + H^{\text{so(tp)}}, \quad (5)$$

$$H^{\text{so(cm)}} = \frac{-\alpha_s(r)}{r^3} \left(\frac{1}{m_2} + \frac{1}{m_1} \right) \left(\frac{\mathbf{S}_1}{m_1} + \frac{\mathbf{S}_2}{m_2} \right) \cdot \mathbf{L} (\mathbf{F}_1 \cdot \mathbf{F}_2) \quad (6)$$

$$H^{\text{so(tp)}} = -\frac{1}{2r} \frac{\partial H^{\text{conf}}}{\partial r} \left(\frac{\mathbf{S}_1}{m_1^2} + \frac{\mathbf{S}_2}{m_2^2} \right) \cdot \mathbf{L}. \quad (7)$$

The spin-orbit interaction will give rise to the mixing between spin singlet 1L_J and spin triplet 3L_J if $m_1 \neq m_2$.

In GI model, the relativistic effects are introduced by two main ways. Firstly, in the quark-antiquark scattering, the interactions should depend on both quark momentum \vec{p}_1 and antiquark momentum \vec{p}_2 , or a linear combination of them as $\vec{p}_1 - \vec{p}_2$ and $\vec{p}_1 + \vec{p}_2$, so they must be nonlocal interaction potentials as pointed out in Ref. [22]. In order to take this effect into account, a smearing function $\rho_{12}(\mathbf{r} - \mathbf{r}')$ is used to transform the basic potentials $G(r)$ and $S(r)$ into the smeared ones $\tilde{G}(r)$ and $\tilde{S}(r)$, the specific form is

$$\tilde{f}(r) = \int d^3r' \rho_{12}(\mathbf{r} - \mathbf{r}') f(r'), \quad (8)$$

and the smearing function $\rho_{12}(\mathbf{r} - \mathbf{r}')$ is defined as

$$\rho_{12}(\mathbf{r} - \mathbf{r}') = \frac{\sigma_{12}^3}{\pi^{3/2}} e^{-\sigma_{12}^2(\mathbf{r} - \mathbf{r}')^2}, \quad (9)$$

$$\sigma_{12}^2 = \sigma_0^2 \left[\frac{1}{2} + \frac{1}{2} \left(\frac{4m_1 m_2}{(m_1 + m_2)^2} \right)^4 \right] + s^2 \left(\frac{2m_1 m_2}{m_1 + m_2} \right)^2. \quad (10)$$

For a heavy-heavy $Q\bar{Q}$ meson system, $\rho_{12}(\mathbf{r} - \mathbf{r}')$ will turn into delta function $\delta^3(\mathbf{r} - \mathbf{r}')$ as one increases the quark mass m_Q , in this case, one can obtain $\tilde{f}(r) = f(r)$, which indicates that the relativistic effects can be neglected for a heavy-heavy $Q\bar{Q}$ meson. However, the relativistic effects are important for heavy-light mesons and light mesons, therefore, it is necessary to consider relativistic effects in the study of excited ρ mesons.

Secondly, the momentum-dependent factors are introduced to modify the effective potentials, as shown in the following formula,

$$\tilde{G}(r) \rightarrow \left(1 + \frac{p^2}{E_1 E_2} \right)^{1/2} \tilde{G}(r) \left(1 + \frac{p^2}{E_1 E_2} \right)^{1/2}, \quad (11)$$

$$\frac{\tilde{V}_i(r)}{m_1 m_2} \rightarrow \left(\frac{m_1 m_2}{E_1 E_2} \right)^{1/2 + \epsilon_i} \frac{\tilde{V}_i(r)}{m_1 m_2} \left(\frac{m_1 m_2}{E_1 E_2} \right)^{1/2 + \epsilon_i}, \quad (12)$$

where $\tilde{G}(r)$ is the Coulomb-type potential, and $\tilde{V}_i(r)$ represents the contact, tensor, vector spin-orbit and scalar

spin-orbit terms as explained in Ref. [22]. In the non-relativistic limit, those momentum-dependent factors will become unity.

With the help of the detailed expressions of Eq. (??), we obtain the mass spectrum and wave functions of mesons by solving the Schrödinger equation with the Gaussian expansion method, the meson wave functions are used as inputs to investigate the subsequent strong decays for mesons.

B. MGI model involving the screening effects

In GI model, linear potential br tends to infinity with the increasing of the distance between quark and antiquark, however for the large distance, the quark-antiquark pairs are generated in the vacuum, and the colors of quark and antiquark are screened in a meson, which implies that the simple linear potential br cannot accurately describe the interaction between quarks for higher excited mesons [26–29]. The study of the lattice QCD shows that the effective potential of mesons deviates from the traditional linear potential when the distance between quark and antiquark is greater than 1 fm [30]. Therefore, it is very important to introduce the screening effects when studying the masses of higher radial and orbital excited mesons.

The screening effects are introduced to the GI model by substituting linear potential br with the following form [26–28],

$$V(r) = br \rightarrow V^{\text{scr}}(r) = \frac{b(1 - e^{-\mu r})}{\mu}, \quad (13)$$

when r is small enough, we can have $V^{\text{scr}}(r) = V(r)$, therefore, this replacement will not affect the lower-lying meson states. The parameter μ is related to the strength of the screening effects and can be determined by fitting to the experimental data.

Furthermore, the smeared potential of Eq.(8) can be rewritten as [28, 31],

$$\begin{aligned} \tilde{V}^{\text{scr}}(r) = & \frac{b}{\mu r} \left[e^{\frac{\mu^2}{4\sigma^2} + \mu r} \left(\frac{1}{\sqrt{\pi}} \int_0^{\frac{\mu + 2r\sigma^2}{2\sigma}} e^{-x^2} dx - \frac{1}{2} \right) \right. \\ & \times \frac{\mu + 2r\sigma^2}{2\sigma^2} + r - e^{\frac{\mu^2}{4\sigma^2} - \mu r} \frac{\mu - 2r\sigma^2}{2\sigma^2} \\ & \left. \times \left(\frac{1}{\sqrt{\pi}} \int_0^{\frac{\mu - 2r\sigma^2}{2\sigma}} e^{-x^2} dx - \frac{1}{2} \right) \right], \quad (14) \end{aligned}$$

where $\sigma = \sigma_{12}$ defined in Eq. (10).

The MGI model is widely used in the studies of mass spectrum of heavy-heavy mesons, heavy-light meson and light mesons [12, 15, 23, 28, 31–37]. The parameters of the MGI model are taken from Ref. [23], as tabulated in Table I. The values of other parameters can be found in Ref. [22].

TABLE I. Parameter values in the MGI model [23].

Parameter	Value	Parameter	Value
m_u (GeV)	0.163	s	1.497
m_d (GeV)	0.163	μ (GeV)	0.0635
m_s (GeV)	0.387	ϵ_c	-0.138
b (GeV ²)	0.221	ϵ_{SOV}	0.157
c (GeV)	-0.240	ϵ_{SOS}	0.9726
σ_0 (GeV)	1.799	ϵ_t	0.893

III. 3P_0 STRONG DECAY MODEL

In addition to the mass spectrum, the strong decay properties are crucial for experiments to search for the higher excited ρ mesons. Here, we give a brief introduction of the 3P_0 model which is widely used in studying two-body OZI-allowed strong decays of mesons [8, 34, 38–40].

The 3P_0 model was originally proposed by Micu [41] in 1968, and later it was further developed by Le Yaouanc *et al* [42, 43]. 3P_0 model has been considered as an effective tool to study two-body OZI-allowed strong decays of hadrons. For the process $A \rightarrow B + C$, the main idea of 3P_0 model is that a flavor-singlet and color-singlet quark-antiquark pair with $J^{PC} = 0^{++}$ is created from the vacuum firstly, then, the created antiquark (quark) combines with the quark (antiquark) in meson A to form meson $B(C)$ as shown in Fig. 1(a) and Fig. 1(b).

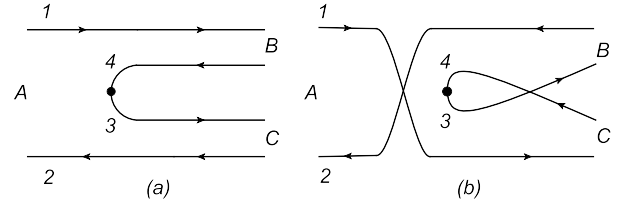


FIG. 1. Two possible diagrams contributing to the process $A \rightarrow B + C$ in the 3P_0 model.

The transition operator T of the decay $A \rightarrow B + C$ in the 3P_0 model is given by [44],

$$\begin{aligned} T = & -3\gamma \sum_m \langle 1m1 - m | 00 \rangle \int d^3\mathbf{p}_3 d^3\mathbf{p}_4 \delta^3(\mathbf{p}_3 + \mathbf{p}_4) \\ & \times \mathcal{Y}_1^m \left(\frac{\mathbf{p}_3 - \mathbf{p}_4}{2} \right) \chi_{1,-m}^{34} \phi_0^{34} \omega_0^{34} b_3^\dagger(\mathbf{p}_3) d_4^\dagger(\mathbf{p}_4), \quad (15) \end{aligned}$$

where $\mathbf{p}_3(\mathbf{p}_4)$ is the momentum of the created quark (antiquark). The dimensionless parameter γ stands for the strength of the quark-antiquark $q_3\bar{q}_4$ pair created from the vacuum, and is usually determined by fitting to the experimental data. $\chi_{1,-m}^{34}$, ϕ_0^{34} and ω_0^{34} are spin, flavor, and color wave functions of the created quark-antiquark pair, respectively.

With the transition operator T , the helicity amplitude $\mathcal{M}^{M_{J_A} M_{J_B} M_{J_C}}(\mathbf{P})$ can be written as,

$$\langle BC|T|A\rangle = \delta^3(\mathbf{P}_A - \mathbf{P}_B - \mathbf{P}_C) \mathcal{M}^{M_{J_A} M_{J_B} M_{J_C}}(\mathbf{P}), \quad (16)$$

where $|A\rangle$, $|B\rangle$ and $|C\rangle$ denote the mock meson states defined in Ref. [45], and \mathbf{P} is the momentum of meson B in the center of mass frame. Then the helicity amplitude is obtained as,

$$\begin{aligned} \mathcal{M}^{M_{J_A} M_{J_B} M_{J_C}}(\mathbf{P}) &= \gamma \sqrt{8E_A E_B E_C} \sum_{\substack{M_{L_A}, M_{S_A}, \\ M_{L_B}, M_{S_B}, \\ M_{L_C}, M_{S_C}, m}} \langle L_A M_{L_A} S_A M_{S_A} | J_A M_{J_A} \rangle \\ &\times \langle L_B M_{L_B} S_B M_{S_B} | J_B M_{J_B} \rangle \langle L_C M_{L_C} S_C M_{S_C} | J_C M_{J_C} \rangle \\ &\times \langle 1m1 - m | 00 \rangle \langle \chi_{S_B M_{S_B}}^{14} \chi_{S_C M_{S_C}}^{32} | \chi_{S_A M_{S_A}}^{12} \chi_{1-m}^{34} \rangle \\ &\times [f_1 I(\mathbf{P}, m_1, m_2, m_3) + (-1)^{1+S_A+S_B+S_C} \\ &\times f_2 I(-\mathbf{P}, m_2, m_1, m_3)], \end{aligned} \quad (17)$$

where $f_1 = \langle \phi_B^{14} \phi_C^{32} | \phi_A^{12} \phi_0^{34} \rangle$ and $f_2 = \langle \phi_B^{32} \phi_C^{14} | \phi_A^{12} \phi_0^{34} \rangle$ correspond to the flavor superposition of the two combinations depicted in Fig. 1(a) and Fig. 1(b), respectively. The momentum space integral $I(\mathbf{P}, m_1, m_2, m_3)$ is given by

$$\begin{aligned} I(\mathbf{P}, m_1, m_2, m_3) &= \int d^3 \mathbf{p} \psi_{n_B L_B M_{L_B}}^* \left(\frac{m_3}{m_1 + m_3} \mathbf{P}_B + \mathbf{p} \right) \\ &\times \psi_{n_C L_C M_{L_C}}^* \left(\frac{m_3}{m_2 + m_3} \mathbf{P}_B + \mathbf{p} \right) \\ &\times \psi_{n_A L_A M_{L_A}}(\mathbf{P}_B + \mathbf{p}) \mathcal{Y}_1^m(\mathbf{p}). \end{aligned} \quad (18)$$

Furthermore, the partial wave amplitude $\mathcal{M}^{LS}(\mathbf{P})$ for the decay $A \rightarrow B + C$ can be expressed as [46],

$$\begin{aligned} \mathcal{M}^{LS}(\mathbf{P}) &= \sum_{\substack{M_{J_B}, M_{J_C}, \\ M_S, M_L}} \langle L M_L S M_S | J_A M_{J_A} \rangle \\ &\times \langle J_B M_{J_B} J_C M_{J_C} | S M_S \rangle \\ &\times \int d\Omega Y_{LM_L}^* \mathcal{M}^{M_{J_A} M_{J_B} M_{J_C}}(\mathbf{P}). \end{aligned} \quad (19)$$

Finally, within the relativistic phase space, the total width $\Gamma(A \rightarrow B + C)$ can be expressed in terms of the partial wave amplitude squared [44],

$$\Gamma(A \rightarrow B + C) = \frac{\pi |\mathbf{P}|}{4M_A^2} \sum_{LS} |\mathcal{M}^{LS}(\mathbf{P})|^2, \quad (20)$$

where $|\mathbf{P}| = \frac{\sqrt{[M_A^2 - (M_B + M_C)^2][M_A^2 - (M_B - M_C)^2]}}{2M_A}$, M_A , M_B , and M_C are the masses of the mesons A , B and C , respectively.

IV. NUMERICAL RESULTS

A. Mass spectrum analysis

First, we have calculated the masses of the higher excited ρ mesons within the MGI and GI models, which are shown in Table II. There are six higher excited ρ mesons in the region of 2.4 ~ 3.0 GeV, which are $\rho(5^3 S_1)$, $\rho(6^3 S_1)$, $\rho(7^3 S_1)$, $\rho(4^3 D_1)$, $\rho(5^3 D_1)$, and $\rho(6^3 D_1)$. The deviations between the predictions of MGI and GI models are about 300 ~ 500 MeV, which implies the screening potential plays an important role in studying the masses of the higher excited ρ mesons.

TABLE II. Masses of the higher excited ρ mesons predicted by the GI and MGI models.

State	MGI (MeV)	GI (MeV)
$\rho(5^3 S_1)$	2542	2817
$\rho(6^3 S_1)$	2774	3160
$\rho(7^3 S_1)$	2967	3470
$\rho(4^3 D_1)$	2624	2915
$\rho(5^3 D_1)$	2840	3239
$\rho(6^3 D_1)$	3020	3554

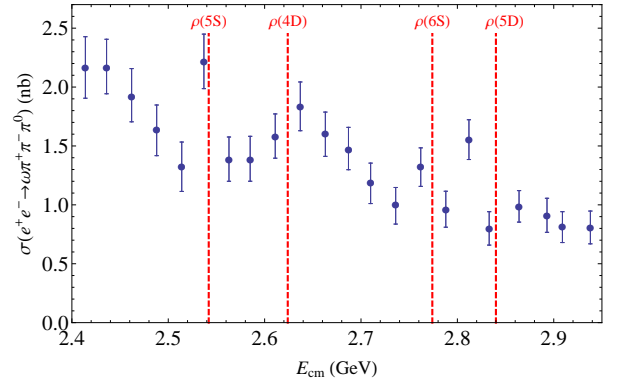


FIG. 2. Comparison of the masses of the higher excited ρ mesons predicted by MGI model with the cross section of the process $e^+e^- \rightarrow \omega\pi^+\pi^-\pi^0$ reported by *BABAR*. The red dotted lines are masses predicted with MGI model, and the blue data points are the *BABAR* experimental data.

The recent analyses of the *BABAR* measurements about the process $e^+e^- \rightarrow K^+K^-\pi^+\pi^-\pi^0$ indicate the existence of one resonance with mass $M = (2550 \pm 13)$ MeV [20], which is in good agreement with our predicted mass of $\rho(5^3 S_1)$. In addition, the cross section of the process $e^+e^- \rightarrow \omega\pi^+\pi^-\pi^0$ measured by *BABAR* indicates that there are hints of the higher excited ρ mesons. From Fig. 2, one can find one datum point around 2.54 GeV, very close to our predicted mass 2542 MeV of $\rho(5^3 S_1)$, and an enhancement structure around 2.64 GeV, which could be related to state $\rho(4^3 D_1)$.

with mass of 2624 MeV. Another datum point appears around 2.76 GeV, close to the predicted mass of $\rho(6^3S_1)$. Although some hints of the higher excited ρ mesons exist, one can not claim those resonances due to the poor quality of the present data, and the more accurate measurements in future are crucial to confirm the existence of these resonances.

In addition, the light mesons with different radial excitation could be well fit to the following quasi-linear (n, M^2) Regge trajectories [47],

$$M_n^2 = M_0^2 + (n-1)\mu^2, \quad (21)$$

where M_n stands for the mass of the meson with radial quantum number n , and M_0^2 and μ^2 are the parameters of the trajectories. With the assignments of $\rho(770)$ as $\rho(1^3S_1)$, $\rho(1450)$ as $\rho(2^3S_1)$, $\rho(1900)$ as $\rho(3^3S_1)$, $\rho(1700)$ as $\rho(1^1D_1)$, and $Y(2040)$ as $\rho(2^3D_1)$, respectively, we plot the Regge trajectories in Fig. 3, where one can find that the masses of $\rho(5^3S_1)$, $\rho(6^3S_1)$, $\rho(7^3S_1)$, $\rho(4^3D_1)$, $\rho(5^3D_1)$, and $\rho(6^3D_1)$ predicted by MGI model are consistent with the estimations of Regge trajectories.

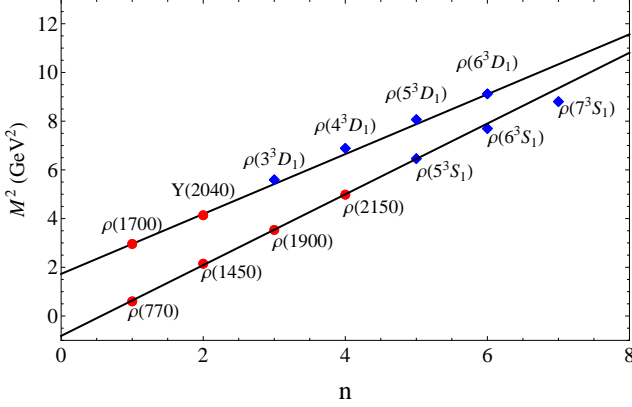


FIG. 3. The Regge trajectories for the $\rho(n^3S_1)$ and $\rho(n^3D_1)$ masses.

B. Decay behavior analysis

In this work, we employ the 3P_0 model with the realistic meson wave functions obtained from the MGI model to evaluate the decay widths of $\rho(5^3S_1)$, $\rho(4^3D_1)$, $\rho(6^3S_1)$, $\rho(5^3D_1)$, $\rho(7^3S_1)$, and $\rho(6^3D_1)$. The value of parameter γ is taken from our previous work [15], where it was obtained by fitting to the decay widths of the light mesons with same quantum numbers as ρ mesons. $\gamma = 6.57$ is used for the $u\bar{u}/d\bar{d}$ pair creation, and the γ value of $s\bar{s}$ pair creation is suppressed by an additional factor m_u/m_s . The predicted masses by the MGI model are used for the unobserved excited ρ mesons in the calculations of the strong decay widths, and the masses of the other mesons are taken from Review of Particle Physics (RPP) [3].

TABLE III. The decay widths of $\rho(5^3S_1)$ (in MeV), the initial state mass is set to be 2542 MeV and the masses of the final states are taken from RPP [3].

Channel	Mode	$\rho(5^3S_1)$	Mode	$\rho(5^3S_1)$
$1^- \rightarrow 0^- 0^-$	$\pi\pi$	2.52	KK	<0.01
	$\pi\pi(1300)$	12.71	$KK(1460)$	0.01
	$\pi\pi(1800)$	9.28		
$1^- \rightarrow 0^- 1^-$	$\pi\omega$	0.81	$KK^*(1680)$	0.01
	$\rho\eta$	0.03	$\rho(1700)\eta$	0.09
	$\omega(1420)\pi$	11.07	$\rho\eta(1475)$	0.17
	$\omega(1650)\pi$	0.11	$\omega\pi(1300)$	1.02
	KK^*	0.02	$\rho\eta(1295)$	0.67
	$KK^*(1410)$	<0.01	$\rho(1450)\eta$	0.65
	$\rho\eta'$	0.14		
$1^- \rightarrow 1^- 1^-$	$\rho\rho$	5.64	K^*K^*	0.15
	$\rho\rho(1450)$	12.93	$K^*K^*(1410)$	0.49
$1^- \rightarrow 0^- 1^+$	$a_1(1260)\pi$	3.26	$b_1(1235)\eta'$	0.17
	$h_1(1170)\pi$	4.22	$\pi a_1(1640)$	9.81
	$KK_1(1400)$	0.10	$b_1(1235)\eta$	0.49
	$KK_1(1270)$	0.10		
$1^- \rightarrow 0^- 2^+$	$a_2(1320)\pi$	4.83	$a_2(1700)\pi$	27.80
	$KK_2^*(1430)$	0.01		
$1^- \rightarrow 0^- 2^-$	$\pi\pi_2(1670)$	3.65	$\pi\eta_2(1645)$	1.94
	$KK_2(1770)$	0.02	$KK_2(1820)$	0.03
$1^- \rightarrow 0^- 3^-$	$\pi\omega_3(1670)$	2.46	$\eta\rho_3(1690)$	0.02
	$KK_3(1780)$	<0.01		
$1^- \rightarrow 1^- 1^+$	$b_1(1235)\rho$	3.38	$K_1(1400)K^*$	0.02
	$a_1(1260)\omega$	3.14	$K_1(1270)K^*$	0.09
	$\rho f_1(1285)$	3.00	$\rho f_1(1420)$	0.16
	$\rho h_1(1170)$	2.50		
$1^- \rightarrow 2^+ 1^-$	$\rho f_2(1270)$	3.93	$K^*K_2^*(1430)$	0.03
	$\omega a_2(1320)$	5.10		
$1^- \rightarrow 0^- 4^+$	$a_4(1970)\pi$	0.91		
$1^- \rightarrow 1^- 0^+$	$a_0(1450)\omega$	0.52		
Total width	143.01			

The partial widths and total width of $\rho(5^3S_1)$ are listed in Table III. The total decay width of $\rho(5^3S_1)$ is expected to be $\Gamma = 143$ MeV, which is close to the lower limit of the width $\Gamma = (209 \pm 26)$ MeV obtained in Ref. [20]. The main decay modes of $\rho(5^3S_1)$ are $\pi\pi(1300)(\rightarrow 4\pi)$, $\pi\pi(1800)(\rightarrow 4\pi)$, $\pi\omega(1420)(\rightarrow 4\pi, 6\pi)$, $\rho\rho(1450)(\rightarrow 4\pi, 6\pi)$, $\pi a_1(1640)(\rightarrow 4\pi)$, and $\pi a_2(1700)(\rightarrow \eta\pi\pi, \pi K\bar{K})$, thus one can search for the $\rho(5^3S_1)$ in the channels of 4π , 6π , $\eta\pi\pi$, and $\pi K\bar{K}$.

The partial widths and total width of $\rho(4^3D_1)$ are listed in Table IV. The total decay width of $\rho(4^3D_1)$ is expected to be $\Gamma = 105.82$ MeV, consistent with the broad structure around 2.64 GeV in Fig. 2. The predicted main decay modes are $\pi\pi(1300)(\rightarrow 4\pi)$, $\pi\pi(1800)(\rightarrow 4\pi)$, $\rho\rho(1450)(\rightarrow 4\pi)$, $\pi h_1(1170)(\rightarrow 4\pi)$, $\pi a_1(1640)(\rightarrow 4\pi)$,

TABLE IV. The decay widths of $\rho(4^3D_1)$ (in MeV), the initial state mass is set to be 2624 MeV and the masses of all the final states are taken from PRR [3].

Channel	Mode	$\rho(4^3D_1)$	Mode	$\rho(4^3D_1)$
$1^- \rightarrow 0^- 0^-$	$\pi\pi$	5.55	KK	<0.01
	$\pi\pi(1300)$	11.16	$KK(1460)$	<0.01
	$\pi\pi(1800)$	7.07		
$1^- \rightarrow 0^- 1^-$	$\pi\omega$	0.48	$KK^*(1680)$	0.01
	$\rho\eta$	0.07	$\rho(1700)\eta$	0.07
	$\omega(1420)\pi$	2.23	$\rho\eta(1475)$	<0.01
	$\omega(1650)\pi$	0.23	$\omega\pi(1300)$	0.61
	KK^*	0.01	$\rho\eta(1295)$	0.36
	$KK^*(1410)$	<0.01	$\rho(1450)\eta$	0.37
	$\rho\eta'$	0.14		
$1^- \rightarrow 1^- 1^-$	$\rho\rho$	4.81	K^*K^*	0.02
	$\rho\rho(1450)$	14.42	$K^*K^*(1410)$	0.06
$1^- \rightarrow 0^- 1^+$	$a_1(1260)\pi$	4.00	$b_1(1235)\eta'$	0.10
	$h_1(1170)\pi$	6.90	$\pi a_1(1640)$	10.54
	$KK_1(1400)$	0.04	$b_1(1235)\eta$	0.82
	$KK_1(1270)$	0.05		
$1^- \rightarrow 0^- 2^+$	$a_2(1320)\pi$	0.96	$a_2(1700)\pi$	7.09
	$KK_2^*(1430)$	<0.01		
$1^- \rightarrow 0^- 2^-$	$\pi\pi_2(1670)$	6.02	$\pi\eta_2(1645)$	4.48
	$KK_2(1770)$	0.05	$KK_2(1820)$	0.01
$1^- \rightarrow 0^- 3^-$	$\pi\omega_3(1670)$	1.35	$\eta\rho_3(1690)$	0.10
	$KK_3(1780)$	<0.01		
$1^- \rightarrow 1^- 1^+$	$b_1(1235)\rho$	1.15	$K_1(1400)K^*$	0.04
	$a_1(1260)\omega$	0.39	$K_1(1270)K^*$	0.08
	$\rho f_1(1285)$	0.52	$\rho f_1(1420)$	0.14
	$\rho h_1(1170)$	1.14		
$1^- \rightarrow 2^+ 1^-$	$\rho f_2(1270)$	5.71	$K^*K_2^*(1430)$	0.01
	$\omega a_2(1320)$	3.58		
$1^- \rightarrow 0^- 4^+$	$a_4(1970)\pi$	0.40		
$1^- \rightarrow 1^- 0^+$	$a_0(1450)\omega$	0.60		
Total width	105.82			

and $\pi\pi_1(1670)(\rightarrow 4\pi)$, thus one can search for $\rho(4^3D_1)$ in the 4π channel.

The partial widths and total width of $\rho(6^3S_1)$ are listed in Table V. The total decay width of $\rho(6^3S_1)$ is expected to be $\Gamma = 67.46$ MeV, and the main decay modes are predicted to be $\pi\pi(1300)(\rightarrow 4\pi)$, $\pi\pi(1800)(\rightarrow 4\pi)$, $\rho\rho(1450)(\rightarrow 4\pi, 6\pi)$, $\pi a_2(1700)(\rightarrow \eta\pi\pi, \pi K\bar{K})$, $\rho f_2(1270)(\rightarrow 4\pi)$, and $\omega a_2(1320)$. Considering the width of the intermediate state $a_2(1320)$ is 107 ± 5 MeV, the $\rho(6^3S_1)$ state is expected to be observed in the $\omega a_2(1320)$ channel.

The partial widths and total width of $\rho(5^3D_1)$ are listed in Table VI. The total decay width of $\rho(5^3D_1)$ is expected to be $\Gamma = 59.00$ MeV, and the predicted main decay modes are $\pi\pi(1300)(\rightarrow 4\pi)$, $\pi\pi(1800)(\rightarrow 4\pi)$,

TABLE V. The decay widths of $\rho(6^3S_1)$ (in MeV), the initial state mass is set to be 2774 MeV and the masses of all the final states are taken from RPP [3].

Channel	Mode	$\rho(6^3S_1)$	Mode	$\rho(6^3S_1)$
$1^- \rightarrow 0^- 0^-$	$\pi\pi$	0.51	KK	<0.01
	$\pi\pi(1300)$	4.83	$KK(1460)$	<0.01
	$\pi\pi(1800)$	5.36		
$1^- \rightarrow 0^- 1^-$	$\pi\omega$	<0.01	$KK^*(1680)$	<0.01
	$\rho\eta$	0.02	$\rho(1700)\eta$	0.04
	$\omega(1420)\pi$	3.29	$\rho\eta(1475)$	0.12
	$\omega(1650)\pi$	0.03	$\omega\pi(1300)$	0.21
	KK^*	<0.01	$\rho\eta(1295)$	0.14
	$KK^*(1410)$	0.01	$\rho(1450)\eta$	0.10
	$\rho\eta'$	0.08		
$1^- \rightarrow 1^- 1^-$	$\rho\rho$	3.67	K^*K^*	<0.01
	$\rho\rho(1450)$	7.26	$K^*K^*(1410)$	0.10
$1^- \rightarrow 0^- 1^+$	$a_1(1260)\pi$	0.59	$b_1(1235)\eta'$	0.09
	$h_1(1170)\pi$	0.79	$\pi a_1(1640)$	5.44
	$KK_1(1400)$	0.02	$b_1(1235)\eta$	0.08
	$KK_1(1270)$	0.02		
$1^- \rightarrow 0^- 2^+$	$a_2(1320)\pi$	0.36	$a_2(1700)\pi$	13.82
	$KK_2^*(1430)$	<0.01		
$1^- \rightarrow 0^- 2^-$	$\pi\pi_2(1670)$	0.95	$\pi\eta_2(1645)$	0.59
	$KK_2(1770)$	<0.01	$KK_2(1820)$	<0.01
$1^- \rightarrow 0^- 3^-$	$\pi\omega_3(1670)$	0.63	$\eta\rho_3(1690)$	<0.01
	$KK_3(1780)$	<0.01		
$1^- \rightarrow 1^- 1^+$	$b_1(1235)\rho$	2.57	$K_1(1400)K^*$	<0.01
	$a_1(1260)\omega$	1.78	$K_1(1270)K^*$	0.01
	$\rho f_1(1285)$	1.68	$\rho f_1(1420)$	0.10
	$\rho h_1(1170)$	1.94		
$1^- \rightarrow 2^+ 1^-$	$\rho f_2(1270)$	4.12	$K^*K_2^*(1430)$	<0.01
	$\omega a_2(1320)$	4.36		
$1^- \rightarrow 0^- 4^+$	$a_4(1970)\pi$	1.31		
$1^- \rightarrow 1^- 0^+$	$a_0(1450)\omega$	0.36		
Total width	67.46			

$\rho\rho(1450)(\rightarrow 4\pi)$, and $\pi a_1(1640)(\rightarrow 4\pi)$. Thus $\rho(5^3D_1)$ is expected to be observed in 4π channel.

The partial widths and total width of $\rho(7^3S_1)$ are listed in Table VII. The total decay width of $\rho(7^3S_1)$ is expected to be $\Gamma = 61.37$ MeV, and the predicted main decay modes are $\pi\pi(1300)(\rightarrow 4\pi)$, $\pi\pi(1800)(\rightarrow 4\pi)$, $\rho\rho(\rightarrow 4\pi)$, $\rho\rho(1450)(\rightarrow 4\pi, 6\pi)$, $\pi a_2(1700)(\rightarrow 4\pi)$, $\pi a_1(1640)(\rightarrow 4\pi)$, and $\omega a_2(1320)$. Thus one can search for the $\rho(7^3S_1)$ state in the $\omega a_2(1320)$ and 4π channels.

The partial widths and total width of $\rho(6^3D_1)$ are listed in Table VIII. The total decay width of $\rho(6^3D_1)$ is expected to be $\Gamma = 23.88$ MeV, and the predicted main decay modes are $\pi\pi(1300)(\rightarrow 4\pi)$, $\pi\pi(1800)(\rightarrow 4\pi)$, $\pi a_1(1640)(\rightarrow 4\pi)$, and $\pi a_2(1700)(\rightarrow 4\pi)$. The state $\rho(6^3D_1)$ is expected to be observed in the 4π channel.

TABLE VI. The decay widths of $\rho(5^3D_1)$ (in MeV), the initial state mass is set to be 2840 MeV and the masses of the final states are taken from RPP [3].

Channel	Mode	$\rho(5^3D_1)$	Mode	$\rho(5^3D_1)$
$1^- \rightarrow 0^- 0^-$	$\pi\pi$	3.46	KK	<0.01
	$\pi\pi(1300)$	10.25	$KK(1460)$	<0.01
	$\pi\pi(1800)$	7.90		
$1^- \rightarrow 0^- 1^-$	$\pi\omega$	0.04	$KK^*(1680)$	0.10
	$\rho\eta$	<0.01	$\rho(1700)\eta$	0.07
	$\omega(1420)\pi$	1.19	$\rho\eta(1475)$	0.01
	$\omega(1650)\pi$	0.20	$\omega\pi(1300)$	0.17
	KK^*	<0.01	$\rho\eta(1295)$	0.11
	$KK^*(1410)$	0.02	$\rho(1450)\eta$	0.10
	$\rho\eta'$	0.04		
$1^- \rightarrow 1^- 1^-$	$\rho\rho$	0.58	K^*K^*	<0.01
	$\rho\rho(1450)$	5.44	$K^*K^*(1410)$	0.04
$1^- \rightarrow 0^- 1^+$	$a_1(1260)\pi$	1.34	$b_1(1235)\eta'$	0.07
	$h_1(1170)\pi$	2.64	$\pi a_1(1640)$	7.35
	$KK_1(1400)$	0.02	$b_1(1235)\eta$	0.16
	$KK_1(1270)$	0.02		
$1^- \rightarrow 0^- 2^+$	$a_2(1320)\pi$	0.84	$a_2(1700)\pi$	5.81
	$KK_2^*(1430)$	<0.01		
$1^- \rightarrow 0^- 2^-$	$\pi\pi_2(1670)$	1.58	$\pi\eta_2(1645)$	1.68
	$KK_2(1770)$	0.01	$KK_2(1820)$	<0.01
$1^- \rightarrow 0^- 3^-$	$\pi\omega_3(1670)$	0.62	$\eta\rho_3(1690)$	0.03
	$KK_3(1780)$	<0.01		
$1^- \rightarrow 1^- 1^+$	$b_1(1235)\rho$	1.22	$K_1(1400)K^*$	0.01
	$a_1(1260)\omega$	0.69	$K_1(1270)K^*$	0.03
	$\rho f_1(1285)$	0.91	$\rho f_1(1420)$	0.12
	$\rho h_1(1170)$	0.93		
$1^- \rightarrow 2^+ 1^-$	$\rho f_2(1270)$	1.41	$K^*K_2^*(1430)$	<0.01
	$\omega a_2(1320)$	0.84		
$1^- \rightarrow 0^- 4^+$	$a_4(1970)\pi$	0.52		
$1^- \rightarrow 1^- 0^+$	$a_0(1450)\omega$	0.46		
Total width	59.00			

V. SUMMARY AND CONCLUSION

In this work, we present the masses and strong decay widths of the higher excited ρ mesons $\rho(5^3S_1)$, $\rho(4^3D_1)$, $\rho(6^3S_1)$, $\rho(5^3D_1)$, $\rho(7^3S_1)$, and $\rho(6^3D_1)$. The deviations between the theoretical masses predicted with MGI and GI models are about 300 ~ 500 MeV, which implies the screening effects are important for the higher excited ρ mesons. We also show some experimental hints for the existences of the higher excited ρ mesons, and one can not claim these resonances based on the poor measurements at present.

In addition to the masses of the higher excited ρ mesons, the strong decay widths are also calculated, which are $\Gamma_{\rho(5S)} = 143$ MeV, $\Gamma_{\rho(4D)} = 106$ MeV, $\Gamma_{\rho(6S)} = 67$ MeV,

TABLE VII. The decay widths of $\rho(7^3S_1)$ (in MeV), the initial state mass is set to be 2967 MeV and the masses of the final states are taken from RPP [3].

Channel	Mode	$\rho(7^3S_1)$	Mode	$\rho(7^3S_1)$
$1^- \rightarrow 0^- 0^-$	$\pi\pi$	<0.01	KK	<0.01
	$\pi\pi(1300)$	4.24	$KK(1460)$	0.01
	$\pi\pi(1800)$	5.77		
$1^- \rightarrow 0^- 1^-$	$\pi\omega$	0.16	$KK^*(1680)$	<0.01
	$\rho\eta$	0.16	$\rho(1700)\eta$	0.09
	$\omega(1420)\pi$	1.14	$\rho\eta(1475)$	0.12
	$\omega(1650)\pi$	0.16	$\omega\pi(1300)$	<0.01
	KK^*	<0.01	$\rho\eta(1295)$	<0.01
	$KK^*(1410)$	<0.01	$\rho(1450)\eta$	<0.01
	$\rho\eta'$	0.11		
$1^- \rightarrow 1^- 1^-$	$\rho\rho$	6.86	K^*K^*	0.04
	$\rho\rho(1450)$	9.09	$K^*K^*(1410)$	<0.01
$1^- \rightarrow 0^- 1^+$	$a_1(1260)\pi$	1.21	$b_1(1235)\eta'$	0.08
	$h_1(1170)\pi$	0.42	$\pi a_1(1640)$	4.28
	$KK_1(1400)$	0.01	$b_1(1235)\eta$	0.15
	$KK_1(1270)$	0.01		
$1^- \rightarrow 0^- 2^+$	$a_2(1320)\pi$	<0.01	$a_2(1700)\pi$	6.86
	$KK_2^*(1430)$	0.02		
$1^- \rightarrow 0^- 2^-$	$\pi\pi_2(1670)$	0.70	$\pi\eta_2(1645)$	0.55
	$KK_2(1770)$	0.01	$KK_2(1820)$	
$1^- \rightarrow 0^- 3^-$	$\pi\omega_3(1670)$	0.04	$\eta\rho_3(1690)$	0.05
	$KK_3(1780)$	<0.01		
$1^- \rightarrow 1^- 1^+$	$b_1(1235)\rho$	3.09	$K_1(1400)K^*$	<0.01
	$a_1(1260)\omega$	1.92	$K_1(1270)K^*$	<0.01
	$\rho f_1(1285)$	1.57	$\rho f_1(1420)$	0.06
	$\rho h_1(1170)$	3.21		
$1^- \rightarrow 2^+ 1^-$	$\rho f_2(1270)$	4.21	$K^*K_2^*(1430)$	0.02
	$\omega a_2(1320)$	3.72		
$1^- \rightarrow 0^- 4^+$	$a_4(1970)\pi$	0.53		
$1^- \rightarrow 1^- 0^+$	$a_0(1450)\omega$	0.24		
Total width	61.37			

$\Gamma_{\rho(5D)} = 59$ MeV, $\Gamma_{\rho(7S)} = 61$ MeV, and $\Gamma_{\rho(6D)} = 24$ MeV, respectively. According to our theoretical predictions, those states are expected to be observed in the final states of 4π , 6π , $\eta\pi\pi$, $\pi K\bar{K}$, $\omega a_2(1320)$. Our theoretical study on their masses and decay properties should be useful to search for these resonances experimentally.

ACKNOWLEDGEMENTS

This work is supported by the Natural Science Foundation of Henan under Grand No. 222300420554. It is also supported by the Key Research Projects of Henan Higher Education Institutions under No. 20A140027, the Project of Youth Backbone Teachers of Colleges

TABLE VIII. The decay widths of $\rho(6^3D_1)$ (in MeV), the initial state mass is set to be 3020 MeV and the masses of the final states are taken from RPP [3].

Channel	Mode	$\rho(6^3D_1)$	Mode	$\rho(6^3D_1)$
$1^- \rightarrow 0^- 0^-$	$\pi\pi$	0.84	KK	<0.01
	$\pi\pi(1300)$	4.29	$KK(1460)$	<0.01
	$\pi\pi(1800)$	5.22		
$1^- \rightarrow 0^- 1^-$	$\pi\omega$	<0.01	$KK^*(1680)$	<0.01
	$\rho\eta$	0.02	$\rho(1700)\eta$	0.03
	$\omega(1420)\pi$	0.40	$\rho\eta(1475)$	0.03
	$\omega(1650)\pi$	0.06	$\omega\pi(1300)$	0.02
	KK^*	<0.01	$\rho\eta(1295)$	0.01
	$KK^*(1410)$	0.01	$\rho(1450)\eta$	<0.01
	$\rho\eta'$	0.03		
$1^- \rightarrow 1^- 1^-$	$\rho\rho$	0.37	K^*K^*	<0.01
	$\rho\rho(1450)$	0.47	$K^*K^*(1410)$	0.03
$1^- \rightarrow 0^- 1^+$	$a_1(1260)\pi$	0.16	$b_1(1235)\eta'$	0.05
	$h_1(1170)\pi$	0.40	$\pi a_1(1640)$	2.90
	$KK_1(1400)$	<0.01	$b_1(1235)\eta$	<0.01
	$KK_1(1270)$	<0.01		
$1^- \rightarrow 0^- 2^+$	$a_2(1320)\pi$	0.05	$a_2(1700)\pi$	2.93
	$KK_2^*(1430)$	<0.01		
$1^- \rightarrow 0^- 2^-$	$\pi\pi_2(1670)$	0.14	$\pi\eta_2(1645)$	0.16
	$KK_2(1770)$	<0.01	$KK_2(1820)$	<0.01
$1^- \rightarrow 0^- 3^-$	$\pi\omega_3(1670)$	0.10	$\eta\rho_3(1690)$	<0.01
	$KK_3(1780)$	<0.01		
$1^- \rightarrow 1^- 1^+$	$b_1(1235)\rho$	0.91	$K_1(1400)K^*$	<0.01
	$a_1(1260)\omega$	0.97	$K_1(1270)K^*$	<0.01
	$\rho f_1(1285)$	0.98	$\rho f_1(1420)$	0.07
	$\rho h_1(1170)$	0.77		
$1^- \rightarrow 2^+ 1^-$	$\rho f_2(1270)$	0.37	$K^*K_2^*(1430)$	<0.01
	$\omega a_2(1320)$	0.05		
$1^- \rightarrow 0^- 4^+$	$a_4(1970)\pi$	0.31		
$1^- \rightarrow 1^- 0^+$	$a_0(1450)\omega$	0.27		
Total width	23.88			

and Universities of Henan Province (2020GGJS017), the Youth Talent Support Project of Henan (2021HYTP002), the Fundamental Research Cultivation Fund for Young Teachers of Zhengzhou University (JC202041042), and the Open Project of Guangxi Key Laboratory of Nuclear Physics and Nuclear Technology, No.NLK2021-08.

-
- [1] M. Ablikim *et al.* [BESIII], Measurement of $e^+e^- \rightarrow K^+K^-$ cross section at $\sqrt{s} = 2.00 - 3.08$ GeV, Phys. Rev. D **99** (2019) no.3, 032001.
- [2] M. Ablikim *et al.* [BESIII], Observation and study of the decay $J/\psi \rightarrow \phi\eta\eta'$, Phys. Rev. D **99** (2019) no.11, 112008.
- [3] P. A. Zyla *et al.* [Particle Data Group], Review of Particle Physics, PTEP **2020** (2020) no.8, 083C01.
- [4] B. Aubert *et al.* [BaBar], Measurements of $e^+e^- \rightarrow K^+K^-\eta$, $K^+K^-\pi^0$ and $K_s^0K^\pm\pi^\mp$ cross-sections using initial state radiation events, Phys. Rev. D **77** (2008), 092002.
- [5] M. Ablikim *et al.* [BESIII], Observation of a resonant structure in $e^+e^- \rightarrow \omega\eta$ and another in $e^+e^- \rightarrow \omega\pi^0$ at center-of-mass energies between 2.00 and 3.08 GeV, Phys. Lett. B **813** (2021), 136059.
- [6] M. Ablikim *et al.* [BESIII], Partial-wave analysis of $J/\psi \rightarrow K^+K^-\pi^0$, Phys. Rev. D **100** (2019) no.3, 032004.
- [7] J. P. Lees *et al.* [BaBar], Resonances in e^+e^- annihilation near 2.2 GeV, Phys. Rev. D **101** (2020) no.1, 012011.
- [8] J. C. Feng, X. W. Kang, Q. F. Lü and F. S. Zhang, Possible assignment of excited light 3S_1 vector mesons, Phys. Rev. D **104** (2021) no.5, 054027.
- [9] L. M. Wang, J. Z. Wang and X. Liu, Toward $e^+e^- \rightarrow \pi^+\pi^-$ annihilation inspired by higher ρ mesonic states around 2.2 GeV, Phys. Rev. D **102** (2020) no.3, 034037.
- [10] P. Masjuan, E. Ruiz Arriola and W. Broniowski, Reply to ‘‘Comment on ‘Systematics of radial and angular-

- momentum Regge trajectories of light nonstrange $q\bar{q}$ -states' ", Phys. Rev. D **87** (2013) no.11, 118502.
- [11] C. Q. Pang, Y. R. Wang, J. F. Hu, T. J. Zhang and X. Liu, Study of the ω meson family and newly observed ω -like state $X(2240)$, Phys. Rev. D **101** (2020) no.7, 074022.
 - [12] C. Q. Pang, Excited states of ϕ meson, Phys. Rev. D **99** (2019) no.7, 074015.
 - [13] C. G. Zhao, G. Y. Wang, G. N. Li, E. Wang and D. M. Li, $\phi(2170)(2170)$ production in the process $\gamma p \rightarrow \eta \phi p$, Phys. Rev. D **99** (2019) no.11, 114014.
 - [14] L. Y. Xiao, X. Z. Weng, X. H. Zhong and S. L. Zhu, A possible explanation of the threshold enhancement in the process $e^+e^- \rightarrow \Lambda\bar{\Lambda}$, Chin. Phys. C **43** (2019) no.11, 113105.
 - [15] Z. Y. Li, D. M. Li, E. Wang, W. C. Yan and Q. T. Song, Assignments of the $Y(2040)$, $\rho(1900)$, and $\rho(2150)$ in the quark model, Phys. Rev. D **104** (2021) no.3, 034013.
 - [16] A. Hasan and D. V. Bugg, Amplitudes for $\bar{p}p \rightarrow \pi\pi$ from 0.36 GeV/c to 2.5 GeV/c, Phys. Lett. B **334** (1994), 215-219.
 - [17] A. V. Anisovich, C. A. Baker, C. J. Batty, D. V. Bugg, L. Montanet, V. A. Nikonov, A. V. Sarantsev, V. V. Sarantsev and B. S. Zou, Combined analysis of meson channels with $I = 1$, $C = -1$ from 1940 to 2410 MeV, Phys. Lett. B **542** (2002), 8-18.
 - [18] B. Aubert *et al.* [BaBar], The $e^+e^- \rightarrow 3(\pi^+\pi^-), 2(\pi^+\pi^-\pi^0)$ and $K^+K^-2(\pi^+\pi^-)$ cross sections at center-of-mass energies from production threshold to 4.5-GeV measured with initial-state radiation, Phys. Rev. D **73** (2006), 052003.
 - [19] B. Aubert *et al.* [BaBar], The $e^+e^- \rightarrow 2(\pi^+\pi^-)\pi^0, 2(\pi^+\pi^-)\eta, K^+K^-\pi^+\pi^-\pi^0$ and $K^+K^-\pi^+\pi^-\eta$ Cross Sections Measured with Initial-State Radiation, Phys. Rev. D **76** (2007), 092005 [erratum: Phys. Rev. D **77** (2008), 119902].
 - [20] P. Lichard, Common explanation of the behavior of some e^+e^- annihilation processes around $\sqrt{s} = 1.9$ GeV, Phys. Rev. D **98** (2018) no.11, 113011.
 - [21] L. M. Wang, S. Q. Luo and X. Liu, Light unflavored vector meson spectroscopy around the mass range of 2.4~3 GeV and possible experimental evidence, Phys. Rev. D **105** (2022) no.3, 034011.
 - [22] S. Godfrey and N. Isgur, Mesons in a Relativized Quark Model with Chromodynamics, Phys. Rev. D **32** (1985), 189-231.
 - [23] C. Q. Pang, J. Z. Wang, X. Liu and T. Matsuki, A systematic study of mass spectra and strong decay of strange mesons, Eur. Phys. J. C **77** (2017) no.12, 861.
 - [24] Q. F. Lü and D. M. Li, Understanding the charmed states recently observed by the LHCb and BaBar Collaborations in the quark model, Phys. Rev. D **90** (2014) no.5, 054024.
 - [25] Q. F. Lü, T. T. Pan, Y. Y. Wang, E. Wang and D. M. Li, Excited bottom and bottom-strange mesons in the quark model, Phys. Rev. D **94** (2016) no.7, 074012.
 - [26] K. T. Chao, Y. B. Ding and D. H. Qin, Possible phenomenological indication for the string Coulomb term and the color screening effects in the quark - anti-quark potential, Commun. Theor. Phys. **18** (1992), 321-326.
 - [27] Y. B. Ding, K. T. Chao and D. H. Qin, Screened Q anti-Q potential and spectrum of heavy quarkonium, Chin. Phys. Lett. **10** (1993), 460-463.
 - [28] Q. T. Song, D. Y. Chen, X. Liu and T. Matsuki, Charmed-strange mesons revisited: mass spectra and strong decays, Phys. Rev. D **91** (2015), 054031.
 - [29] X. C. Feng, Wei-Hao and I. J. Liu, The assignments of the bottom mesons within the screened potential model and 3P_0 model, [arXiv:2205.07169 [hep-ph]].
 - [30] K. D. Born, E. Laermann, N. Pirch, T. F. Walsh and P. M. Zerwas, Hadron Properties in Lattice QCD With Dynamical Fermions, Phys. Rev. D **40** (1989), 1653-1663.
 - [31] Q. T. Song, D. Y. Chen, X. Liu and T. Matsuki, Higher radial and orbital excitations in the charmed meson family, Phys. Rev. D **92** (2015) no.7, 074011.
 - [32] J. Z. Wang, D. Y. Chen, X. Liu and T. Matsuki, Constructing J/ψ family with updated data of charmonium-like Y states, Phys. Rev. D **99** (2019) no.11, 114003.
 - [33] J. Z. Wang, Z. F. Sun, X. Liu and T. Matsuki, Higher bottomonium zoo, Eur. Phys. J. C **78** (2018) no.11, 915.
 - [34] W. Hao, G. Y. Wang, E. Wang, G. N. Li and D. M. Li, Canonical interpretation of the $X(4140)$ state within the 3P_0 model, Eur. Phys. J. C **80** (2020) no.7, 626.
 - [35] T. G. Li, Z. Gao, G. Y. Wang, D. M. Li, E. Wang and J. Zhu, The possible assignments of the scalar $K_0^*(1950)$ and $K_0^*(2130)$ within the 3P_0 model, [arXiv:2203.17082 [hep-ph]].
 - [36] Z. Gao, G. Y. Wang, Q. F. Lü, J. Zhu and G. F. Zhao, Canonical interpretation of the $Ds_0(2590)^+$ resonance, Phys. Rev. D **105** (2022) no.7, 074037.
 - [37] C. Q. Pang, Y. R. Wang and C. H. Wang, Prediction for 5^{++} mesons, Phys. Rev. D **99** (2019) no.1, 014022.
 - [38] T. T. Pan, Q. F. Lü, E. Wang and D. M. Li, Strong decays of the $X(2500)$ newly observed by the BESIII Collaboration, Phys. Rev. D **94** (2016) no.5, 054030.
 - [39] G. Y. Wang, S. C. Xue, G. N. Li, E. Wang and D. M. Li, Strong decays of the higher isovector scalar mesons, Phys. Rev. D **97** (2018) no.3, 034030.
 - [40] S. C. Xue, G. Y. Wang, G. N. Li, E. Wang and D. M. Li, The possible members of the 5^1S_0 meson nonet, Eur. Phys. J. C **78** (2018) no.6, 479.
 - [41] L. Micu, Decay rates of meson resonances in a quark model, Nucl. Phys. B **10** (1969), 521-526.
 - [42] A. Le Yaouanc, L. Oliver, O. Pene and J. C. Raynal, Naive quark pair creation model of strong interaction vertices, Phys. Rev. D **8** (1973), 2223-2234.
 - [43] A. Le Yaouanc, L. Oliver, O. Pene and J. C. Raynal, Naive quark pair creation model and baryon decays, Phys. Rev. D **9** (1974), 1415-1419.
 - [44] H. G. Blundell, Meson properties in the quark model: A look at some outstanding problems, arXiv:hep-ph/9608473 [hep-ph].
 - [45] C. Hayne and N. Isgur, Beyond the Wave Function at the Origin: Some Momentum Dependent Effects in the Nonrelativistic Quark Model, Phys. Rev. D **25** (1982), 1944.
 - [46] M. Jacob and G. C. Wick, On the General Theory of Collisions for Particles with Spin, Annals Phys. **7** (1959), 404-428.
 - [47] A. V. Anisovich, V. V. Anisovich and A. V. Sarantsev, Systematics of $q\bar{q}$ states in the (n, M^2) and (J, M^2) planes, Phys. Rev. D **62** (2000), 051502.

